5.11.2. — zmęczenie
5.11.7. — ośrodki nieliniowe sprężyste i lepkosprężyste
5.11.12. — badania doświadczalne

Zdzisław Świderski

TESTING OF THE FRACTURE RESISTANCE OF RAILS

5/1994

WARSZAWA 1994

ISSN 0208-5658

Praca wpłynęła do Redakcji dnia 19 listopada 1994 r.

IPPT PAN

Na prawach rękopisu

Instytut Podstawowych Problemów Techniki PAN
Nakład 100 egz. Ark.wyd. 1,00 Ark.druk. 1,5
Oddano do drukarni w styczniu 1994 r.

Wydawnictwo Spółdzielcze sp. z o.o.
Warszawa, ul.Jasna 1

Zdzisław Świderski
Samodzielna Pracownia
Dynamiki i Stateczności
Maszyn i Pojazdów
IPPT PAN Warszawa

TESTING OF THE FRACTURE RESISTANCE OF RAILS

SUMMARY

Various grades of rail steel as well as whole rail sections were subjected to fracture resistance tests according to the unified method. It was found that heat treatment of rails (pearlitization) increased fracture resistance by 50%, however, residual stresses had also substantial effect. Apparent durability values Nc from the Wilson formula have been derived. The influence of residual stresses to rail durability was stated.

1. INTRODUCTION

Fatigue brittle fractures of rails experienced during their operational use on the track produce considerable threat to passengers' safety. Durability of rails was much improved when heavy track structures using the UIC60 type rails (made of St 90 AP higher-strength steel of R_m tensile strength not less than 880 MPa) were introduced. At present, rails of this type are made of converter steel and manufactured by the Huta Katowice. Although, quality of these rails represents modern European standard, tough operational conditions existing in the PKP network (traffic load is several times larger than that of West European railways) result in continued defects of rails (e.g. longitudinal cracks of webs due to excessive residual stress after straightening,

contact chipping, or the so called shelling, premature wear of rails on bends, transverse fatigue brittle cracks, cracks due to the holes to fix joint bars).

Therefore, extensive research work regarding an analysis of wide range of physical properties of the rail which may have an effect on its durability and reliability was undertaken.*

2. OBJECTIVES

The aim of this work was to:

a/ establish a method and procedure of testing,

b/ find correlation between resistance to cracking and other properties of rail steels,

c/ determine factors influencing increase in resistance of rails to cracking.

3. SCOPE

In the first stage, unused rails manufactured by leading European steel mills (including the Huta Katowice) were tested. In the second stage, rails excluded from operation due to fatigue cracking of brittle nature were examined (including 5 rails removed from the Polish tracks). Methods of testing employed by several European research establishments were unified, so was location, shape and execution of specimen.

This paper presents test results for two grades of higher wear resistance rail steel manufactured by the Huta Katowice: 110 CrNb low-alloy steel, and quenched and tempered 90 PA steel (by through hardening at 860°C in the OH80 oil at 80 – 100°C and tempering in the oven at 450°C for 1 hour), also 5 UIC 60 rails made of St 90

* The Author has been a member of the team which carried out the tests for the D 156 Expert Committee of the European Research Railway Institute, results of which are presented in this paper.

A and B steel by the Huta Kościuszko in 1972. They had been removed from the PKP track after 10 years of service, due to transverse fatigue brittle cracks.

4. TEST RESULTS

4.1. Chemical composition

Following the tensile tests the specimen were subjected to chemical analysis (16 components) using the ARL 31000 Spectrometer.

Chemical composition of the first steel (St 110 Cr-Nb) corresponds with low-alloy chromium rail steel with addition of niobium. Rails of increased wear resistance, made of this steel have been manufactured by the Huta Katowice since 1983. Second steel, shown in the tables, features chemical composition corresponding with the St 90 AP converter rail steel – regularly manufactured by the Huta Katowice. However, rail sections have been subjected to heat treatment – so called pearlitization according to the above process which Huta Katowice implemented in 1985.

Five rails which have been removed from the track are of the Huta Kościuszko make. Four of them feature chemical composition corresponding with the St 90 AP rail steel, one (No. 197.120) – with the St 90 BP steel (increased manganese contents). As regards chemical composition, all of them comply with the requirements of both the Polish Standard PN-H/93421 and the International Standard UIC-860.

4.2. Mechanical properties

Mechanical properties have been determined using standard specimens cut out from both the rail head and foot. Impact tests were carried out at various temperatures (from -40°C to +60°C) – while certain specimens were tested at temperatures between -60°C and +140°C, on specimen with a Mesnager notch (r = 1 mm) 2 mm deep (KMU 2), also on the removed from the track DVMF specimen, with the 4 mm deep notch of r = 4 mm. Measured energies (J) referring to the DVMF specimens

are given in brackets. Test results are shown in Table 1. The values represent averages of three specimens.

4.3. Fracture toughness (K_{IC})

Fracture toughness was determined using the KF 20 specimen according to the ASTM-E 399 Standard [1]; specimens (of a thickness B = 20 mm and height W = 40 mm) were cut out from the rail head (Fig. 1) and subjected to three point bending test. Growth of the fatigue crack (a) was performed using the Instron 1251 machine by applying cyclic loading until crack size of a = 20 mm was obtained.

Values of K_{IC} fracture toughness have been determined from the formula:

$$K_Q = \frac{4P_Q}{B\sqrt{W}} f\left(\frac{a}{W}\right) \tag{1}$$

Value of the function $f(a/W)$ were taken from the table provided in the Standard [1]. K_Q preliminary value is considered as the K_{IC} fracture toughness provided that the following conditions of two-dimensional state of deformation are satisfied:

1) $a > 2{,}5\ (K_Q/R_e)^2$ and the pattern of front of the crack is uniform over entire cross section

2) $B > 2{,}5\ (K_Q/R_e)^2$

3) $P_{max}/P_Q < 1{,}1$

Test results are presented in the Table 2. As regards certain specimen, the conditions 2/ or 3/ have not been satisfied (see the remarks in the Table 2). Therefore the calculated value of K_Q may not be recognized as K_{IC}.

Specific fracture energy $(U/B)_c$ according to the IRSid method [2] was also determined. Static bend test of the ISO-V impact specimen was carried out. Their K_{IC} can be determined from the formula:

$$\left(\frac{U}{B}\right)_c = \frac{\alpha(1-\nu^2)(W-a)}{2E} K_{IC}^2 \tag{2}$$

following substitution of the following values:

$\nu = 0{,}3$;

$E = 206\,000$ MPa;

$B = W = 10$ mm;

$W - a = 8$ mm;

α = coefficient of notch reaction;

$\alpha = 15$ for the ISOV specimen;

$$K_{IC} = 61{,}3 \sqrt{\left(\frac{U}{B}\right)_C} \tag{3}$$

The results of this test (U/B) - for new rails, together with calculated values of K_{IC} are shown in Table 2.

4.4. Fatigue crack growth rates

Fatigue crack growth rates were determined using the AF25 specimens (thickness B = 20 mm, height W = 50 mm) extracted from rail heads in the same way as described above (Fig. 1). Fatigue crack growth was developed under three point bend conditions, as for determination of K_{IC}, under the load of P_{max} = 12 kN, R = 0,1, and f = 20 Hz. Crack width increments were measured every 0,5 mm and increment in number of load cycles was recorded. Coefficient of stress intensity $\Delta K_i = \Delta\sigma\sqrt{a_i M_i}$ was calculated for each measurement.

Results are shown in Fig. 2. Paris equation coefficients [3]

$$\frac{dN}{da} = C_o \Delta K^n \tag{4}$$

i.e. C_o and n material constants were determined according to the least square method. The results are presented in Table 2.

4.5. Distribution of residual stresses

Distribution of residual stresses over the rail section was determined using three sectioning techniques.

Method A – strain gauges of 10 mm datum were fixed to rail section periphery - longitudinally and transversely, as shown in Fig. 3. Gauges were zeroed upon their connection with the measuring bridges. Then, a 20 mm thick slice with fixed strain gauges was machine sawn out. Stress increment readings were taken from each gauge when the segment cooled down. Next, cubes with strain gauges were cut out from the slice and stress increment was measured.

Method B – Surfaces of terminal sections of 0,4 m long rail piece were face ground. Along vertical axis of symmetry, measuring points were centre-punched every 10 mm on both parallel sections. Zeiss measuring machine was used to measure distances between points – with an accuracy of 0,001 mm. Then, the rail piece was cut up to bars approx. 10 mm across, with measuring points in the middle of their thickness (Fig. 4), and the bars were again measured using the same measuring machine. Basing on length increase of the bars, longitudinal residual stresses acting at centre-punched points of the rail section were calculated.

Method C – Strain gauges, the same as above, were glued along vertical axis of symmetry of rail profile on axial section of 0.5 m long rail piece (Fig. 5). Axial section was obtained after planing away half the profile all along the rail piece. Similarly, the first measurement was taken after 20 mm thick slice with strain gauges was cut out, second one – after cutting out the cubes.

Distribution of longitudinal residual stresses along the height of the rail is given in Fig. 6. The straightening process of rail causes on appearance of the longitudinal residual stresses of maximal values of the tensile stresses situated close to the head side surface and to the lower surface of the foot. In the web occur selt compensation compression stresses. During on exploatation of the rail in the tracks the initial tensil stresses in the surface layer due to pressure change into compression stresses.

4.6. Fatigue testing of rail sections

Since all basic data regarding material properties as well as magnitude and distribution of residual stresses were available, fatigue tests of entire rail sections (approx. 1,2 m long) using four point bending technique (pure bending) resulting in variable tensile stress in the rail foot (Fig. 7), were commenced. Using 100 mm dia milling cutter, a 22 mm long (length of trace on the foot surface) and 1 mm deep notch, with root radius $r = 0{,}01$ mm, was made in the middle portion of lower surface of the rail foot (Fig. 7). The tests were carried out at constant value of maximum stresses $\sigma_z = 200$ MPa in the notch area (verified by means of the strain gauges fixed around the notch) – at an coefficient of load asymmetry $R = 0{,}1$.

Upon specimen braking, critical size of the fatigue crack was measured (Fig. 8). Critical fatigue crack size is characterized by the two parameters: critical crack depth a_c [mm] and critical crack length 2c – developing from the notch root.

If the crack length 2c is less than 22 mm, i. e. less than the length of the notch, Rail Fracture Resistance (K_{RFR}) is calculated basing on the effective crack length 2c' i. e. after its extension down to lower edge of the foot according to the arc of a circle circumscribed on the actual crack.

Rail fracture resistance K_{RFR} was calculated from the formula given by Irwin [4] for bending of a plate with elliptical surface crack of a depth a:

$$K_{RFR} = \frac{F\sigma_z\sqrt{\pi a}}{\sqrt{Q}} \qquad [\text{MPa}\sqrt{\text{m}}] \tag{5}$$

Where: F – stress intensity correction coefficient for given specimen shape;

Q – correction coefficient related to surface cracks of semi-elliptical shape defined by the ratio of their semi-axes a/c;

σ_z – stress produced by an external load (with no regard to magnitude and distribution of residual stresses).

F and Q coefficients have been calculated from the formulae derived by Newman and Raju [5] using finite element method for the deepest point of a crack on the plate

subjected to bending - at the moment of a brittle crack. Plate thickness t was substituted by the height of the UIC60 rail profile b = 172 mm – for brand new rails. As regards used rails, their heights B were measured and given in Table 3. Since F = f (a/c,a/B) and Q = f (a/c), function $Y = \frac{F}{\sqrt{Q}}$ was tabulated as shown in Fig. 9. Results of tests and calculations of K_{RFR} are given in Table 3. In calculations of critical crack intensity coefficient K_{CS} at the deepest point of a fatigue crack, σ_w residual stress and external load generated stress σ_z – acting in the middle of critical crack depth:

$$K_{CS} = \frac{M_S \left[\frac{(B-a)}{B} \sigma_z + 0{,}88\ \sigma_w \left(1 - \frac{\frac{a}{2}}{23{,}4} \right) \right] \sqrt{\pi a}}{\sqrt{Q}} \tag{6}$$

Where, for the UIC 60 rails:

$$M_S = 1{,}12 - 0{,}09 \left(\frac{a}{c} \right) \tag{7}$$

$$\sqrt{Q} = \sqrt{1 + 1{,}464\ (a/c)^{1{,}65}} \tag{8}$$

Value of the residual stress σ_w was obtained from the reading of gauge F_1 taken during the measurements of residual stresses carried out according to the method A. Coefficients 0,88 and 23,4 result from the distribution of longitudinal residual stresses in the foot section. As regards the UIC 60 rails, at a depth of approx. 23,4 mm the above stresses change their sign (expectation value). Calculated K_{CS} are presented in Table 3.

If we compare values of rail brittle crack resistance (K_{RFR}), stress intensity coefficient (K_{CS}), and material fracture toughness (K_{IC}), we can notice substantial effect of magnitude of residual stresses (originating from rail strengthening by means of the roller straightener) on durability of rails. This becomes clearly visible when sections of straightened or not straightened (or stress relieved through soaking at 550°C for 3 hours) rails are subjected to fatigue tests. For UIC 60 rail made of 90 AP steel and subjected to bending moment as above, in the same conditions, for

straightened rail (σ_w = 240 MPa) critical fatigue crack of a_c = 4,7 mm, 2c = 20,0 mm was obtained, while for stress relieved section of the same rail: a_c = 13,5 mm, 2c = 31,2 mm.

4.7. Determination of the apparent rail durability

Having calculated, from crack growth rate test, material constants (for 90 AP steel) $C_o = 3.64 \times 10^{-14}$ [m/cyklxMPa$\sqrt{m}$], and the exponent m = 4,29, we are able to calculate the apparent durability N_c using the Wilson formula [6] derived from integration of the Paris formula (4):

$$N_c = \frac{2\left\{\left(\frac{1}{\frac{(m-2)}{a_o\ 2}} - \frac{1}{\frac{(m-2)}{a_c\ 2}}\right)\right\}}{(m-2)\ C_O\ (\Delta\sigma)^m\ M^{\frac{m}{2}}} \quad \text{[cycles]} \tag{9}$$

If we assume that the notch depth is a_o = 1 mm, then the time of fatigue crack growth represented by number of cycles withstood [M_c] – from the moment of crack formation to sudden fracture – for the relieved rail is N_{co} = 4,043 [Mc] (megacycles), and N_{cw} = 1,025 [Mc] – for straightened rail. (Fig. 10).

5. CONCLUSIONS

5.1. Fatigue test of the rail section with a notch may be suitable for determination of the value of K_{IC} (K_{CS}) provided residual stresses – determined for example by means of the Debro [7] ultrasonic method being a non-destructive test – are known.

5.2. Residual stresses σ_w = 240 MPa, produced during rail straightening process using roller straightener, reduce apparent rail durability four times.

5.3. At the same time, considerable reduction in fatigue crack depth ac (around three times) is visible, while the apparent rail durability is reduced by 4,5 times. Dependence of the apparent rail durability Nc on the size (depth) of the crack ao is shown in Fig. 10. It may be used for comparative evaluation of quality of rails in

respect of their fracture resistance and assessment of menace produced by cracks of particular size.

5.4. Heat treatment (pearlitization) of the rails made of 90 A steel results in an increase of K_{IC} by 50%, so at least twofold service durability of such rails may be expected.

Paper supported by Grant KBN – PB No 3097891.01

REFERENCES

1. ASTM-E399 Standard: Test Method for Plane-Strain Fracture Toughness of Metallic Materials

2. Marandet B.: Evaluation simple de la ténacité pour le suivi de la qualité des materiaux. Rapport IRSid RPF 295 VII 1981

3. Paris P.C., Erdogan F.: Journal of Basic Engineering, Trans ASME 85 Series D 1963 p. 528-534

4. Irwin G.R.: Crack Extension Force for a Part Through Crack in a Plate. ASME Journal of Applied Mecanics XII 1962 p. 651 – 654

5. Newman J.C., Raju I.S.: Analyses of Surface Cracks in Finite Plates Under Tension or Bending Loads. NASA Technical Paper 1578, X 1978

6. Wessel E.T.,Clark W.C., Wilson W.K.:Engineering Methods for the Design and Selection of Materials Against Fracture. John Wiley and Sons. Inc. 1971

7. Deputat J. at al. Experiences in ultrasonic measurement of rail residual stresses – Residual Stress in Rail. O. Orringer, J. Orkisz, Z. Świderski (eds) Kluwer Ac. Publ. 1992 EAFM Ser Vol. 12 p. 169 – 183

Table 1. Mechanical properties of the Polish rails tested

Rail	Grade of Steel	Location of Specimen	Re [MPa]	Rm [MPa]	Re/Rm -	A5 [%]	Z [%]	Impact strength (J) at a temperature of: [°C]									
								-60	-40	-20	0	+20	+60	+80	+100	+120	+140
Alloy steel	110 Cr-Nb	Head	628	1098	0,57	13,7	34,4	5	5,4	4,4	7,3	8	9,7	23,7	23,3	25,3	23,3
		Foot	703	1125	0,63	11,9	29,4	-	-	5,7	9,3	8	-	-	-	-	-
Hardened sections	90 AP	h.	715	1101	0,65	14,1	41,6	19,3	24	24	28,7	30	38,7	48	48	54,7	53,3
	U.C.	f.	574	934	0,61	15,9	37,1	-	-	23,3	28,7	37,3	-	-	-	-	-
Extracted from the track at km: 196 040	90 AP	h.	482	887	0,54	13,1	22,6	-	4,3 /6,9/	7,8 /10,8/	10,3 /15,7/	/19,5/	/26,0/	-	-	-	-
		f.	565	895	0,63	13,4	20,8		6,9 /9,3/	7,8 /11,3/	8,0 /15,5/	/20,4/	/24,0/	-	-	-	-
	196 360	90 AP	h.	515	892	0,58	14,4	26,0		3,9 /3,4/	2,9 /8,0/	3,9 /9,1/	6,8 /15,4/	/25,7/				
			f.	565	895	0,63	14,4	24,3		3,9 /4,4/	4,9 /7,7/	4,4 /6,2/	7,7 /20,6/	/28,3/				
	197 120	90 BP	h.	570	1000	0,57	12,8	18,1		3,9 /4,1/	3,9 /4,1/	6,9 /6,1/	5,5 /8,0/	/12,9/				
			f.	675	1040	0,65	12,6	20,8		3,9 /4,6/	2,9 /4,1/	5,9 /5,1/	/8,3/	/12,6/				
	200 345	90 AP	h.	555	960	0,58	11,8	16,4		3,9 /4,4/	3,9 /5,6/	4,9 /7,3/	6 /11,0/	/17,5/				
			f.	680	955	0,68	10,0	17,2		4,9 /4,4/	5,9 /5,6/	6,9 /6,5/	6,1 /10,3/	/19,0/				
	201-126	90 AP	h.	505	867	0,58	14,2	22,6		3,9 /3,1/	3,9 /5,2/	4,9 /8,2/	7,5 /13,6/	/21,2/				
			f.	545	875	0,62	13,2	22,6		3,4 /3,4/	6,9 /5,7/	7,8 /7,5/	10,0 /12,2/	/24,9/				

Impact resistance values relating to the DVMF are given in brackets

Table 2. Fracture toughness test results (K_{rc}) and crack growth rates (C_o and n constants)

Rail	Grade of Steel	Location of Specimen	a_{or} [mm]	a/W	f/a/	P_Q [kN]	K_Q [MPa$\sqrt{m}$]	$2,5\left(\frac{K_Q}{R_{0,2}}\right)^2$ [m]	Uwagi	K_{IC} [MPa$\sqrt{m}$]	$\left(\frac{U}{B}\right)_C$ [kJ/m]	K^x_{IC} [MPa$\sqrt{m}$]	Average values of K_{rc} or K_a [MPa$\sqrt{m}$]	C_o	n
1	2	3	4	5	6	7	8	9	10	11	12	13	14	15	16
Alloy steel	110CrNb	1 2 Head 3	20,38 19,71 21,31	0,509 0,493 0,532	2,74 2,60 2,95	14,15 14,8 13,9	38,77 38,48 41,00	9,6 9,4 10,7		38,8 38,5 41,0	0,45 0,34 0,42	38,8	39,4	$2,2 \times 10^{-13}$	4,2
Hardened sections	90APU.C	1 2 h. 3	19,83 20,44 20,23	0,496 0,511 0,506	2,63 2,76 2,71	24,2 20,7 20,2	63,65 57,10 60,16	19,8 15,0 17,7	$P_{max} > 1.1 P_Q$ - " - - " -		1,25 1,26 1,03	66,4	60,3	$1,93 \times 10^{-12}$	3,2
196.040	90AP	1 2 h. 3	20,93 21,05 20,88	0,523 0,526 0,522	2,87 2,90 2,86	19,1 20,3 19,5	55,8 58,7 54,8	33,3 37,1 32,3	$D < 2,5\left(\frac{K_Q}{R_{0,2}}\right)^2$ - " - - " -				56,4	$4,63 \times 10^{-17}$ $1,33 \times 10^{-16}$	6,15 6,11
		1 2 Foot 3	20,97 21,73 20,13	0,526 0,546 0,505	2,9 3,1 2,7	16,2 17,0 20,6	47,5 52,8 55,7	17,7 21,9 24,3	- " - - " -	47,5			52,0	-	-
196 360	90AP	1 2 Head 3	20,65 21,23 21,52	0,516 0,531 0,538	2,28 2,95 3,02	19,7 15,0 14,6	55,2 44,3 43,9	29 18 19	- " -	44,3 43,9	-	-	47,8	$3,56 \times 10^{-24}$ $1,19 \times 10^{-20}$	10,4 8,6
197 120	90DP	1 2 h. 3	21,22 21,18 21,22	0,531 0,530 0,531	2,95 2,94 2,95	10,6 10,6 11,5	31,3 33,9 31,2	8 9 9		31,3 33,9 31,2			32,1	$3,51 \times 10^{-28}$ $4,44 \times 10^{-15}$	12,8 4,9
200.345	90AP	1 2 h. 3	21,05 20,08 20,18	0,526 0,502 0,505	2,90 2,68 2,70	13,3 12,2 12,8	32,7 38,6 34,6	12 8 10		32,7 38,6 34,6	-	-	35,3	$2,1 \times 10^{-17}$ $1,32 \times 10^{-20}$	6,43 10,8
201.126	90AP	1 2 h. 3	21,70 20,40 20,07	0,543 0,510 0,502	3,07 2,75 2,68	16,2 18,8 22,6	49,6 51,6 60,4	24 26 26	- " - - " - - " -		-	-	53,9	$4,05 \times 10^{-16}$ $1,77 \times 10^{-16}$	5,5 5,79
		1 2 f. 3	21,46 20,93 20,86	0,546 0,530 0,524	3,1 2,99 2,88	17,16 18,4 18,5	53,9 54,3 53,4	24,1 24,8 24,0	- " - - " - - " -		-	-	53,9	-	-

Extracted from the track at km:

x/ Calculated value of $K_{rc} = 67,3\sqrt{(U/B)}$.

Table 3. Results of fatigue testing of the rail section with a notch

Rail	Grade of Steel	a [mm]	2c [mm]	a' [mm]	B [mm]	σ_{max} [MPa]	K_{RPR} [MPa $\sqrt{m}$]	$\sigma_{w(P4)}$ [MPa]	K_{Cs} [MPa $\sqrt{m}$]	K_{Ic} (K_Q) [MPa $\sqrt{m}$]
1	2	3	4	5	6	7	8	9	10	11
Alloy steel	110 CrMo	5 5,5 2,9	16,2 14,0 18,4	8,5 7,4 10,2	172 172 172	200 200 200	20,6 19,7 23,9	310	34,04 38,16 31,98	39,4
Hardened sections	90APOC	16,1 18,5 18,6	38,7 46,8 47,4	19,4 23,4 23,7	172 172 172	200 200 200	28,8 30,9 31,4	101	35,51 32,95 33,09	(60,3)
Extracted from the track at km: 196.040	90 AP	9,5 8,5 28,4	31,4 24,3 72,1	15,7 12,2 36,1	168 168 168	200 200 200	27,0 24,2 35,2	149	42,2 38,2 48,4	(56,4)
196.360	90 AP	2,5 4,6 4,4	12,1 15,4 16,8	6,6 8,0 8,5	169 169 169	200 200 200	16,8 19,7 20,2	173	28,9 33,8 34,4	44,1
197.120	90 BP	5,5 2,0 2,0	12,2 23,3 19,3	6,3 11,7 10,6	170 170 170	200 200 200	18,2 16,8 16,7	172	30,4 28,9 28,6	32,1
200.345	90 AP	2,2 2,5 2,8	8,6 9,6 10,2	8,2 8,3 6,0	171 171 171	200 200 200	16,8 17,7 16,7	156	27,7 28,9 27,7	35,3
201.126	90 AP	8,9 4,5 7,2	22,7 14,7 14,4	11,4 7,4 7,2	170 170 170	200 200 200	23,7 19,3 18,7	120	34,4 28,7 27,7	(33,9)

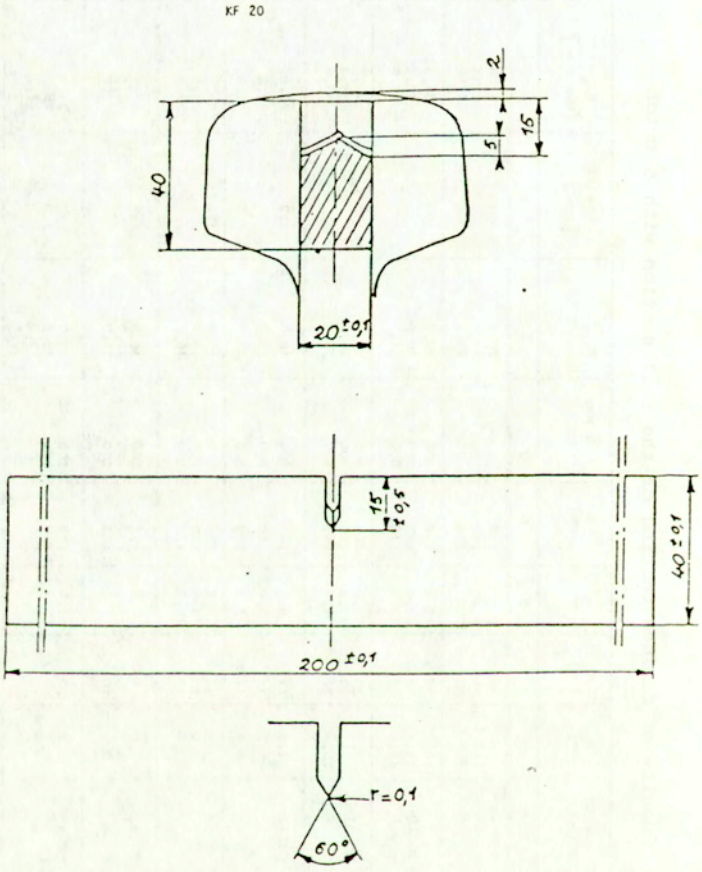

Fig. 1 - Dimensions of the specimen used for determination of K_{Ic} and its location in the rail head

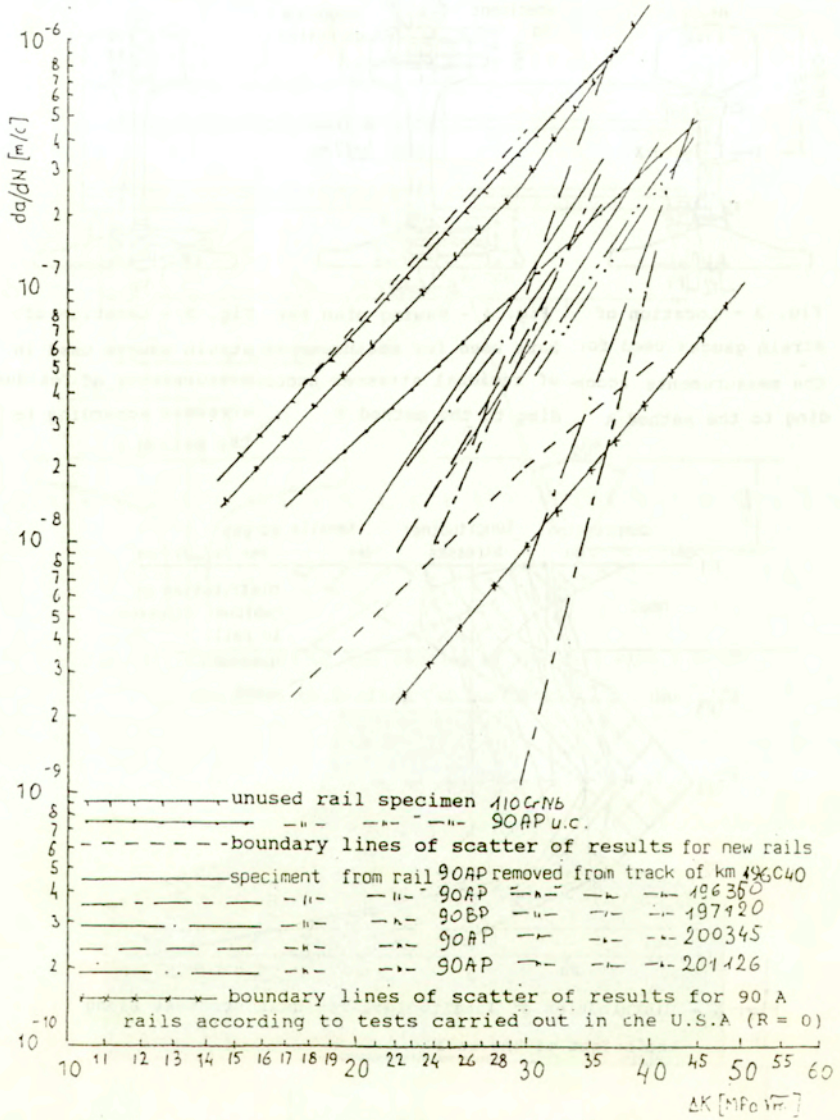

Fig. 2 - Crack growth diagrams for tested rail steels

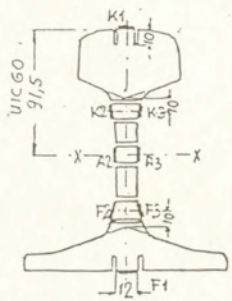

Fig. 3 - Location of strain gauges used for the measurements according to the method A

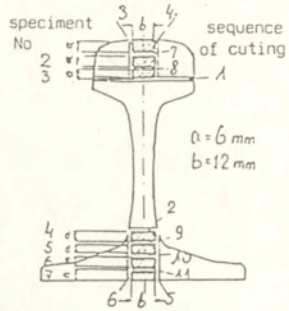

Fig. 4 - Sawing plan for bars used for measurements of residual stresses according to the method B

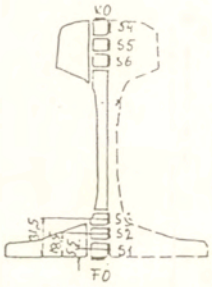

Fig. 5 - Location of strain gauges used in measurements of residual stresses according to the method C

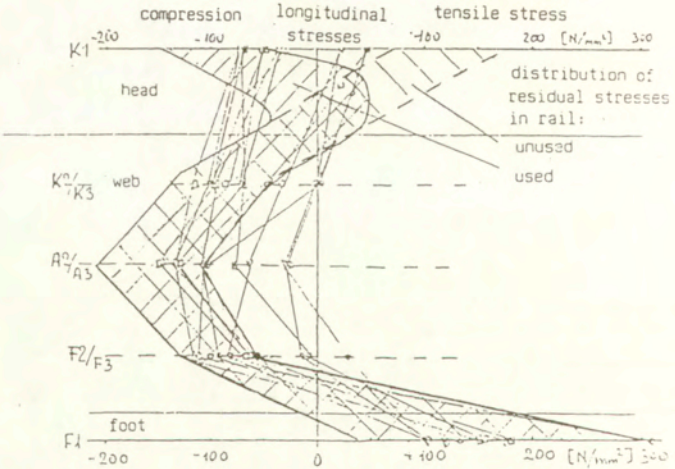

Fig. 6 - Distribution of longitudinal residual stresses along the height of the rail

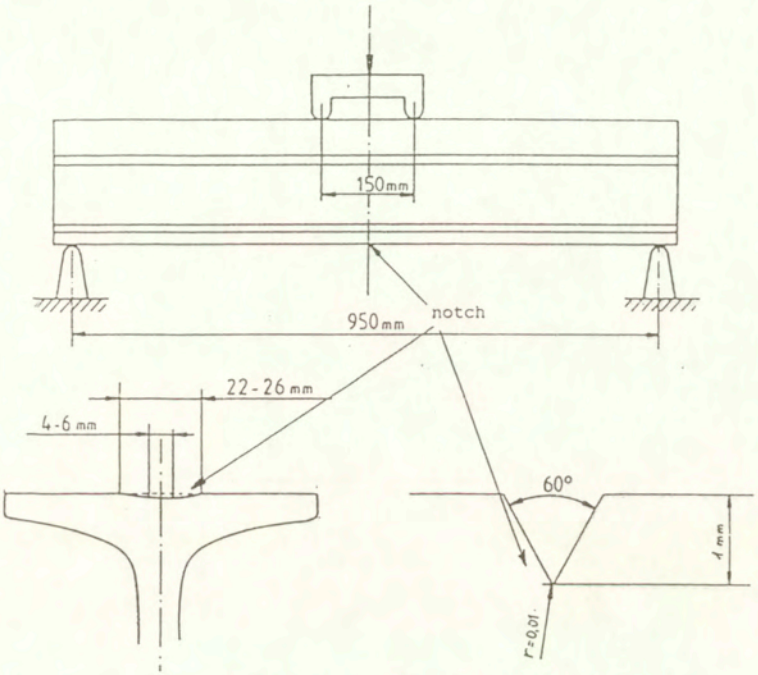

Fig. 7 - Dimensions of the section of the rail with a notch subjected to bending fatigue test

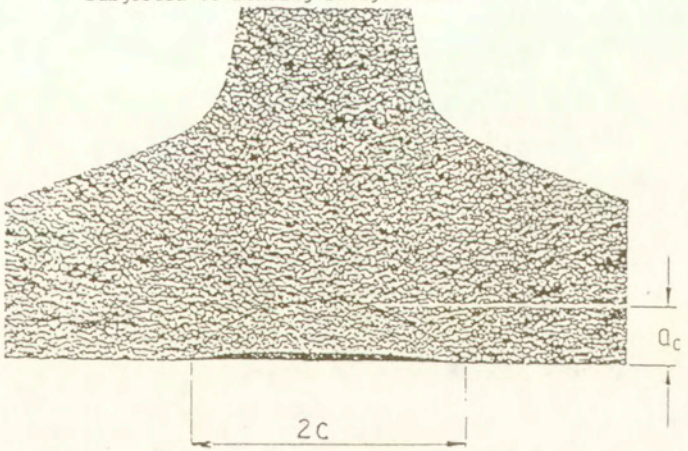

Fig. 8 - Method of measurement of critical size of the fatigue crack

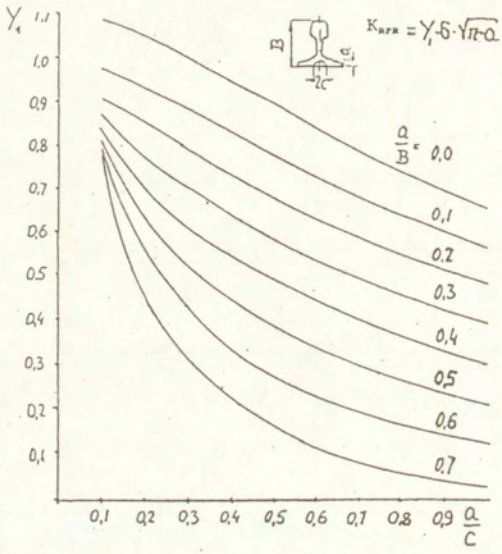

Fig. 9 - Values of the coefficient $Y=F/\sqrt{Q}$ for calculation of K_{ara}

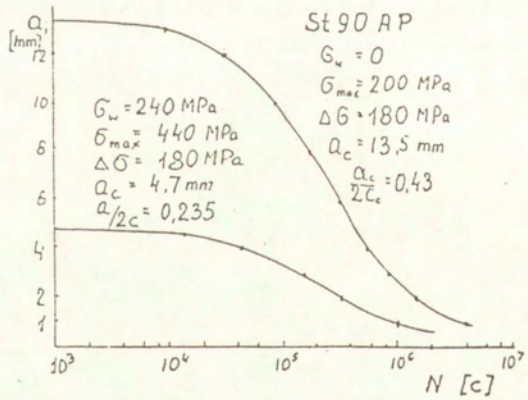

Fig. 10 - Dependence of the apparent durability on the crack size (a_1) for the UIC 60 rail made of 90 AP steel:
- with residual stresses (σ_w = 240 MPa);
- stress relieved (σ_w = 0).